GOSPODARKA SUROWCAMI MINERALNYMI – MINERAL RESOURCES MANAGEMENT

2023 Volume 39 Issue 1 Pages 23–34

DOI: 10.24425/gsm.2023.144633

ZHEHAO WANG[1], LING WANG[2], YUTING HE[3], JIONGRAN DUAN[4], BOWEN FAN[5]

Mineralogy characteristics, stability conditions, and formation pathways of synthetic pyrrhotite formed by heating pyrite at 700°C

Highlights

Synthetic pyrrhotite differs from natural pyrrhotite in the mineral association.
Synthetic pyrrhotite-4C was stable under 0.5–2 h of heating at 700°C in air.
Synthetic pyrrhotite-4C had the largest content at 700°C by heating for 1 hour.
In air, synthetic pyrrhotite-4C is formed mainly via two pathways.
Pyrite → pyrrhotite-4C is the more favorable path of pyrrhotite-4C formation.

✉ Corresponding Author: Ling Wang; e-mail: wangling@cdut.edu.cn
[1] Chengdu University of Technology, China; ORCID iD: 0000-0002-2833-4526; e-mail: wangzhehao@stu.cdut.edu.cn
[2] Chengdu University of Technology, China; ORCID iD: 0000-0002-8588-9149; e-mail: wangling@cdut.edu.cn
[3] Chengdu University of Technology, China; e-mail: hythxq@163.com
[4] Chengdu University of Technology, China; e-mail: 425197085@qq.com
[5] Chengdu University of Technology, China; e-mail: fanbowen0452@126.com

Introduction

Pyrite (FeS_2) is the most common sulfide mineral and is widely distributed in nature (Priestley and Paul 1964; Craig et al. 1998; Kołodziejczyk 2009; Oliveira et al. 2016; Stepanov et al. 2021). As a result of its universality and importance, pyrite has been extensively studied in terms of its mineralogy, thermal decomposition, and mineral transformation (Lambert et al. 1998; Huang and Rowson 2001; Ferrow and Sjöberg 2005; Wang et al. 2014; Huang et al. 2021). When heated at high temperatures, pyrite may transform into ferrimagnetic minerals (e.g. pyrrhotite or magnetite) or canted antiferromagnetic minerals (e.g. hematite) (Li and Zhang 2005; Wang et al. 2008; Bhargava et al. 2009; Shi et al. 2015; Zhang et al. 2019). Understanding these transformation mechanisms can inform important technical approaches for the magnetic separation of pyrite as a paramagnetic mineral.

Pyrrhotite is widely identified in endogenetic deposits and has also been observed in a series of hydrothermal deposits (Matsumoto and Nakamura 2012; Bogdanova et al. 2016; Palyanova et al. 2019; Mansur et al. 2021). Pyrrhotite, like pyrite, is a raw material used in the preparation of sulfuric acid and sulfur. The mineralogical characteristics of natural pyrrhotite have been extensively studied (Kondoro and Kiwanga 1997; Kontny et al. 2000; Wang and Salveson 2005; Selivanov et al. 2008). However, synthetic pyrrhotite, which is formed by heating pyrite in air, has not been sufficiently investigated. It is necessary to study the crystal structure and mineral association differences between synthetic and natural pyrrhotite, as well as the stability conditions of synthetic pyrrhotite at elevated temperatures in air, based on existing research. These investigations will support processing engineering techniques and industrial applications of pyrite and pyrrhotite.

Synthetic pyrrhotite is mainly formed from the oxidation of pyrite at elevated temperatures in air (Wang et al. 2008; Wang et al. 2014). The transformation of pyrite to pyrrhotite is carried out according to the following reaction:

$$7FeS_2\,(s) + 6O_2\,(g) \rightarrow Fe_7S_8\,(s) + 6SO_2\,(g); \quad \Delta H\,(700°C) = -1{,}327.9\ kJ/mol \tag{1}$$

The enthalpy value was calculated by HSC Chemistry 6.0 software. Some possible formation pathways have been proposed by previous studies. For example, small amounts of magnetite may participate in the transformation of pyrite to pyrrhotite (Li and Zhang 2005; Wang et al. 2008):

$$7FeS_2\,(s) \rightarrow Fe_7S_8\,(s) + 6S\,(s); \quad \Delta H\,(700°C) = 528.9\ kJ/mol \tag{2}$$

$$3FeS_2\,(s) + 8O_2\,(g) \rightarrow Fe_3O_4\,(s) + 6SO_2\,(g); \quad \Delta H\,(700°C) = -2{,}362.5\ kJ/mol \tag{3}$$

$$2Fe_3O_4\,(s) + FeS_2\,(s) + 10/nS_n\,(s) \rightarrow Fe_7S_8\,(s) + 4SO_2\,(g); \quad \Delta H\,(700°C) = 302.5\ kJ/mol \tag{4}$$

Small amounts of magnetite cannot be identified by X-ray diffraction (XRD) but can be verified by thermomagnetic curve analysis. According to Wang et al. (Wang et al. 2014), hematite may be further transformed into pyrrhotite in the presence of sulfur produced in reaction (2):

$$4FeS_2\ (s) + 11O_2\ (g) \rightarrow 2Fe_2O_3\ (s) + 8SO_2\ (g); \quad \Delta H\ (700°C) = -3{,}315.0\ kJ/mol \qquad (5)$$

$$14Fe_2O_3\ (s) + 53S\ (s) \rightarrow 4Fe_7S_8\ (s) + 21SO_2\ (g); \quad \Delta H\ (700°C) = 1{,}491.9\ kJ/mol \qquad (6)$$

Possible formation pathway should be verified by subsequent experiments.

In this work, natural pyrite, pyrrhotite, and hematite samples were used for analysis. The synthesis pathway of synthetic pyrrhotite was verified by material synthesis. The crystal structure, mineral association, and formation pathways of pyrrhotite formed by heating pyrite were further examined using XRD.

1. Experimental method

Information on the experimental samples is presented in Table 1. Table 2 provides chemical compositions of natural mineral samples as analyzed through the use of X-ray fluores-

Table 1. Natural mineral samples and reagents from China used in the experiments

Tabela 1. Naturalne próbki minerałów i odczynniki z Chin użyte w doświadczeniach

Minerals	Samples	Chemical formula	Sample characteristics	Location
Pyrrhotite	KW28	$Fe_{1-X}S$	single mineral aggregate	Yuhang, Zhejiang
Pyrite	KW30	FeS_2	single mineral aggregate	Kuandian, Liaoning
Kidney-shaped hematite	KW51	Fe_2O_3	single mineral aggregate	Xuanhua, Hebei
Sulfur		S	AR	Chengdu, Sichuan

Table 2. Chemical compositions (wt.%) of natural mineral samples

Tabela 2. Składy chemiczne (% wag.) naturalnych próbek mineralnych

Minerals	Samples	Fe_2O_3	SO_3	SiO_2	Al_2O_3	CaO	MgO
Pyrrhotite	KW28	32.58	66.38	0.72	0.13	0.19	0
Pyrite	KW30	34.39	64.62	0.74	0.17	0.05	0.03
Kidney-shaped hematite	KW51	76.78	0.03	21.49	1.15	0.32	0.24

cence (XRF). Natural pyrite (KW30) had a pure pyrite phase (Figure 1). As Wang et al. (Wang et al. 2014) reported the highest conversion efficiency from pyrite to pyrrhotite in air at 700°C, sample KW30 was crushed to 40 mesh and heated at 700°C for 0.5–4 h in air prior to further experiments. One sample was weighted for 5 g into a corundum crucible and heated using a muffle furnace. K-type thermocouple was utilized to measure the temperature with a deviation of ±5°C.

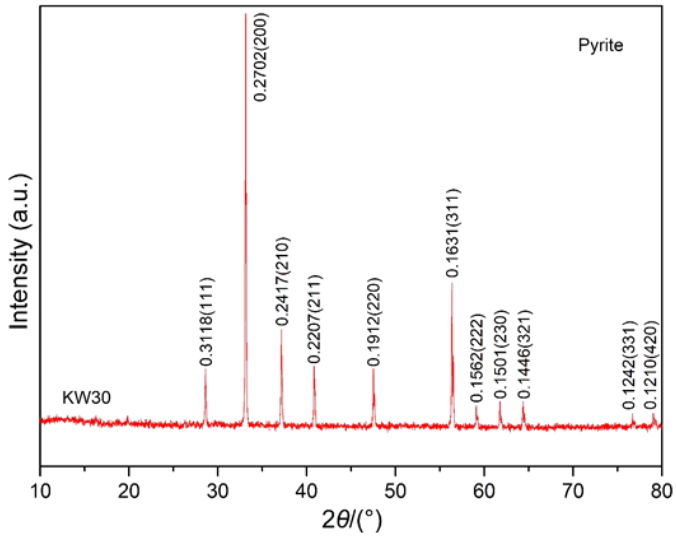

Fig. 1. XRD pattern of natural pyrite (KW30) (modified from Wang et al. 2014)

Rys. 1. Dyfraktogramy XRD naturalnego pirytu (KW30)

Solid-phase reaction experiments for reaction (6) were conducted as follows: natural hematite (KW51) and sulfur were crushed and ground to a 200 mesh size using an agate mortar. They were mixed evenly in a molar ratio of 1:3.8. The mixture was heated at 700°C for 1 h in air.

Powder XRD experiments were performed on a DX-2700 diffractometer (Haoyuan Instrument Co., Ltd., China) to determine the constituent phases of the samples. The diffraction profiles were recorded in the range of 10–80° (2θ) using a step scan technique (1 s per step with an interval of 0.03°) under Cu K_α radiation. The XRD results were analyzed using MDI Jade 6 software with a diffraction standards database (ICDD PDF2 2004).

2. Results and discussion

2.1. Mineralogy characteristics of natural and synthetic pyrrhotite samples

FeS is troilite and is hexagonal; Fe_7S_8 is one of the typical structures of pyrrhotite mineral and is monoclinic pyrrhotite-4C. Pyrrhotites with intermediate compositions (5C, 6C, and their intermediates) are monoclinic but mentioned as pseudohexagonal (Morimoto et al. 1975). As shown in Figure 2, the natural pyrrhotite sample (KW28) has pyrrhotite-4C and magnetite phases as well as unknown phases, causing some unidentified diffraction peaks at 10–13° and 27–29° (2θ). Pyrite products heated at 700°C for 1 h consisted of mainly pyrrhotite-4C and hematite with a small amount of pyrite and magnetite as well as unknown phases inducing diffraction peaks at 25–27° (2θ). There was a difference in the paragenetic association of minerals between natural and synthetic pyrrhotites. The XRD results matched well with those of JCPDS 89-1954, pyrrhotite-4C (Tokonami et al. 1972). Diffraction peaks of (228), (400), (224), (620), (448), and (004) were clearly observed. The *d*-values for the hexagonal form (102), distinct from the monoclinic form (228) of pyrrhotite-4C at 44° (2θ) in this case, were 0.2056 nm for natural pyrrhotite-4C and 0.2054 nm for synthetic pyrrhotite-4C (Figure 2). The values obtained are in good agreement with that of 0.2052 nm obtained from a monoclinic pyrrhotite-4C crystal (Tokonami et al. 1972). This indicates

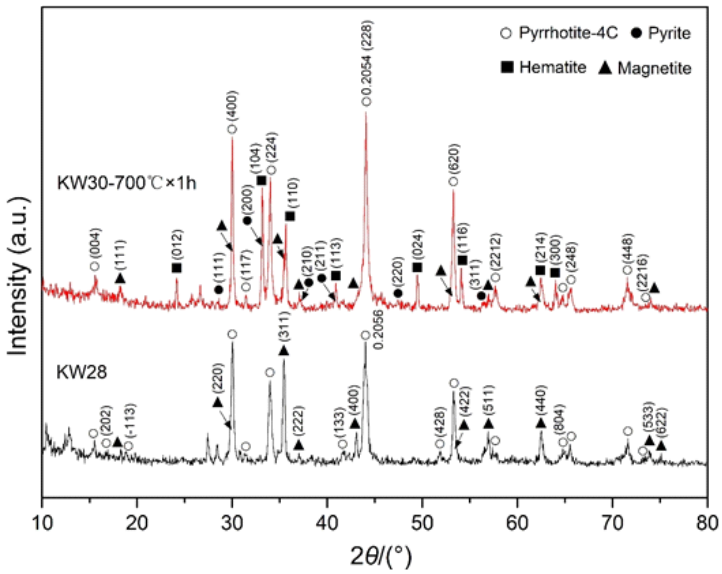

Fig. 2. XRD patterns of natural pyrrhotite (KW28) and synthetic pyrrhotite formed by heating pyrite (KW30) for 1 h at 700°C

Rys. 2. Dyfraktogramy XRD pirotynu naturalnego (KW28) i pirotynu syntetycznego powstałe w wyniku ogrzewania pirytu (KW30) przez 1 h w temperaturze 700°C

that the natural and synthetic pyrrhotites may both be classified as pure pyrrhotite-4C. Table 3 lists the lattice parameters of natural and synthetic pyrrhotite-4C. All samples were monoclinic pyrrhotite-4C (Fe_7S_8) and exhibited minimal differences in terms of lattice parameters.

Table 3. Lattice parameters of natural pyrrhotite (KW28) and synthetic pyrrhotite formed by heating pyrite (KW30) for 1 h at 700°C

Tabela 3. Parametry sieci krystalicznej pirotynu naturalnego (KW28) i pirotynu syntetycznego utworzonego przez ogrzewanie pirytu (KW30) przez 1 h w temperaturze 700°C

Samples	Crystal system	$a \times b \times c$ (nm)	β	V (nm^3)	Z	D
Natural pyrrhotite	Monoclinic	1.1910(7) × 0.6863(4) × 2.2825(13)	90.43(3)°	1.866	8	4.610
Synthetic pyrrhotite	Monoclinic	1.1912(10) × 0.6860(5) × 2.2774(19)	90.44(5)°	1.861	8	4.621

2.2. Stability conditions of synthetic pyrrhotite-4C formed under 700°C in air

According to previous studies, synthetic pyrrhotite formed by heating pyrite at 700°C is stable under argon and nitrogen atmospheres (Li and Zhang 2005; Wang et al. 2008; Bhargava et al. 2009; Shi et al. 2015). However, it is unclear whether synthetic pyrrhotite remains stable in air. At 700°C, synthetic pyrrhotite formed by heating pyrite had the maximum content in air (Wang et al. 2014).

As shown in Figure 3, the pyrite-heated products have the phases of mainly pyrrhotite-4C and hematite when held at 700 °C in air. Synthetic pyrrhotite-4C formed stably by heating pyrite for 0.5–2 h. Its relative content was the highest at 81.8% (Table 4) by heating for 1 h (Figure 4). The percentages of pyrrhotite-4C and hematite were calculated by MDI Jade 6 software. Small amounts of pyrite and magnetite were also observed. However,

Table 4. The percentages (wt.%) of pyrrhotite-4C and hematite in pyrite products by heating at 700°C

Tabela 4. Udziały procentowe (% wag.) pirotynu-4C i hematytu w produktach pirytowych po ogrzaniu w temperaturze 700°C

Heating time	0.5 h	1 h	2 h	3 h	4 h
Pyrrhotite-4C	47.8	81.8	44.2	0	0
Hematite	52.2	18.2	55.8	100	100

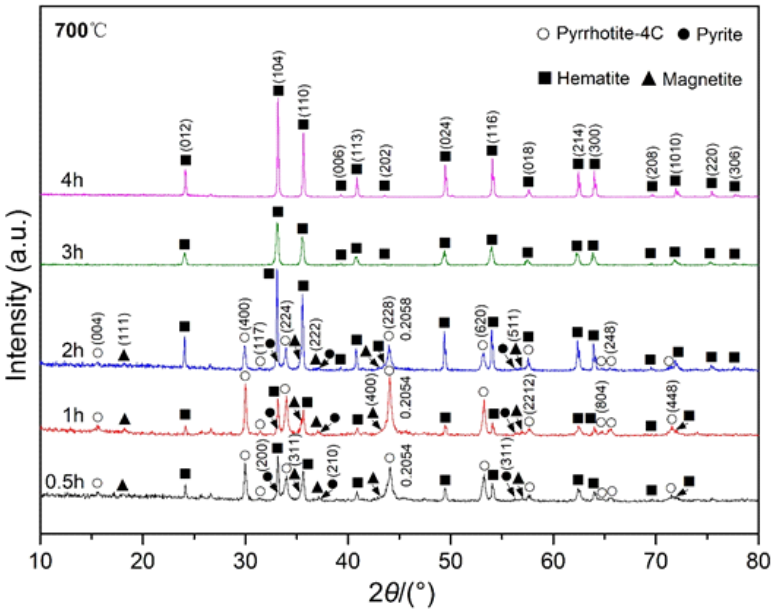

Fig. 3. XRD patterns of pyrite products formed by heating at 700°C for 0.5 to 4 h

Rys. 3. Dyfraktogramy XRD produktów pirytowych powstałych w wyniku ogrzewania w temperaturze 700°C w czasie od 0,5 do 4 godzin

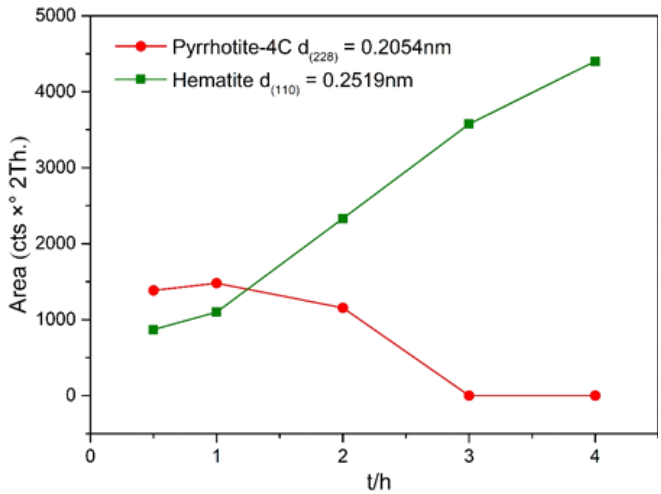

Fig. 4. Integral areas of diffraction peaks of pyrrhotite-4C at d(228) = 0.2054 nm and hematite at d(110) = 0.2519 nm in pyrite products by heating at 700°C for 0.5 to 4 h

Rys. 4. Obszary integralne pików dyfrakcyjnych pirotynu-4C przy d(228) = 0,2054 nm i hematytu przy d(110) = 0,2519 nm w produktach pirytowych po ogrzewaniu w temperaturze 700°C w czasie 0,5 do 4 h

the pyrrhotite-4C phase disappeared completely when the heating period exceeded 3 h, as was the case for pyrite and magnetite. Hematite was the final oxidation product, which is consistent with several previous studies (Wang et al. 2008; Bhargava et al. 2009). Li and Zhang (Li and Zhang 2005) suggested that pyrrhotite is the final product in air. This difference may be due to the creation of an anoxic environment by the slender quartz glass tubes (with an inner diameter of 6.5 mm and length of 177 mm) used in the heating experiments.

It should be noted that the pyrite heating process in this work was always performed in a muffle furnace. Using other type of furnaces, e.g. fluidized bed, microwave furnace, may have different stability conditions for synthetic pyrrhotite-4C in air. This is worthy of further study in future work.

2.3. Formation pathways of synthetic pyrrhotite-4C formed by heating pyrite at 700°C in air

In this study, synthetic pyrrhotite-4C was mainly formed from the oxidation of pyrite in air by reaction (1). There are several possible formation pathways. As illustrated in Figures 2 and 3, the XRD results show that a small amount of magnetite was generated with the formation of synthetic pyrrhotite-4C. Thus, magnetite may participate in the transformation of pyrite to pyrrhotite-4C via reactions (2)–(4). Hematite could be formed from the oxidation of pyrite by reaction (5). The possibility of reaction (6) (hematite to pyrrhotite-4C) was disapproved by a solid-phase reaction. XRD results (Figure 5) show

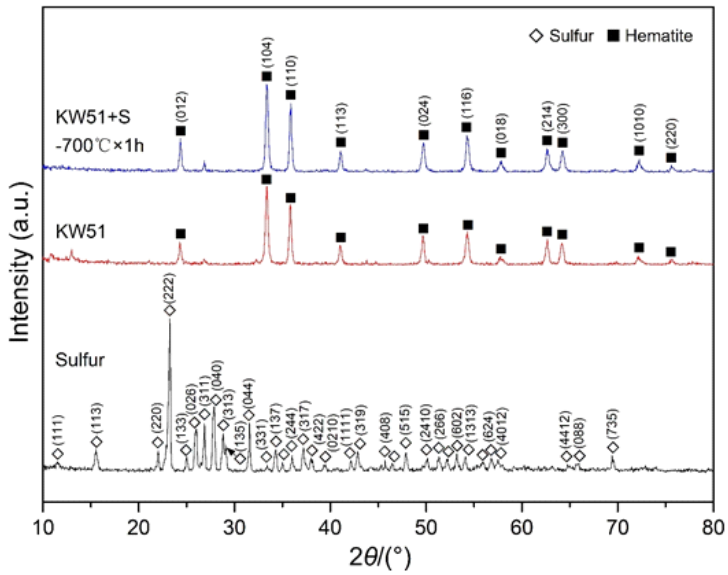

Fig. 5. XRD patterns of the raw materials and products of reaction (6)

Rys. 5. Dyfraktogramy XRD surowców i produktów reakcji (6)

that reaction (6) could not proceed at 700°C in air. By contrast, pyrrhotite-4C was completely transformed into hematite at a heating period longer than 3 h (Figure 3) according to the following reaction:

$$4Fe_7S_8\ (s) + 5_3O_2\ (g) \rightarrow 14Fe_2O_3\ (s) + 32SO_2\ (g); \quad \Delta H\ (700°C) = -17{,}893.6\ kJ/mol \quad (7)$$

Thus, the pyrite specimen (KW30) transformed into pyrrhotite-4C at 700°C in air along two pathways: (1) pyrite → pyrrhotite-4C by reactions (1) or (2); (2) pyrite → magnetite → pyrrhotite-4C by the reactions (2) to (4). Reaction (2) is crucial to pathway (2) but not to pathway (1). Therefore, pathway (1) is more favorable than path (2). Hematite cannot be transformed into pyrrhotite-4C by reaction (6).

Conclusions

Synthetic pyrrhotite, which is formed by heating pyrite at 700°C in air, exhibits a distinct paragenetic association of minerals compared with that of natural pyrrhotite. Natural pyrrhotite and magnetite coexist in the natural pyrrhotite sample, while synthetic pyrrhotite has the paragenetic association with hematite and a small amount of pyrite and magnetite. Both are monoclinic pyrrhotite-4C (Fe_7S_8) and have minimal differences in terms of lattice parameters. Synthetic pyrrhotite-4C forms stably by heating pyrite for 0.5–2 h. Its relative content was the highest by heating for 1 h. However, pyrrhotite-4C would transform into hematite completely when heated for longer than 3 h, as was the case for pyrite and magnetite. In air, synthetic pyrrhotite-4C is formed mainly via two pathways: (1) pyrite → pyrrhotite-4C and (2) pyrite → magnetite → pyrrhotite-4C. Pathway (1) is more favorable than path (2). This transformation cannot be achieved by the reaction between hematite and sulfur.

This work was supported by National Natural Science Foundation of China (No. 41972039, 41572038) and Sichuan Science and Technology Program (2020YFS0391). The authors would like to thank the critical reviews and constructive remarks of the two anonymous reviewers.

REFERENCES

Bhargava et al. 2009 – Bhargava, S.K., Garg, A. and Subasinghe, N.D. 2009. In situ high-temperature phase transformation studies on pyrite. *Fuel* 88, pp. 988–993, DOI: 10.1016/j.fuel.2008.12.005.

Bogdanova et al. 2016 – Bogdanova, O.Y., Lein, A.Y., Dara, O.M., Ozhogina E.G. and Lisitzin A.P. 2016. Pyrrhotite mineralization as a search criterion for sulfide deposits at sediment-covered spreading centers. *Doklady Earth Sciences* 470, pp. 928–932, DOI: 10.1134/S1028334X16090038.

Craig et al. 1998 – Craig, J., Vokes, F. and Solberg, T. 1998. Pyrite: physical and chemical textures. *Mineralium Deposita* 34, pp. 82–101, DOI: 10.1007/s001260050187.

Ferrow, E.A. and Sjöberg, B.A. 2005. Oxidation of pyrite grains: A mössbauer spectroscopy and mineral magnetism study. *Hyperfine Interactions* 163, pp. 95–108, DOI: 10.1007/s10751-005-9199-8.

Huang et al. 2021 – Huang, F., Xin, S.Z., Mi, T. and Zhang L.Q. 2021. Study of pyrite transformation during coal samples heated in CO_2 atmosphere. *Fuel* 292, DOI: 10.1016/j.fuel.2021.120269.

Huang, J.H. and Rowson, N.A. 2001. Heating characteristics and decomposition of pyrite and marcasite in a microwave field. *Minerals Engineering* 14(9), pp. 1113–1117, DOI: 10.1016/S0892-6875(01)00117-0.

Kołodziejczyk, U. 2009. Hydrological, geological and geochemical conditions determining reclamation of post - mine land in the region of Łęknica. *Gospodarka Surowcami Mineralnymi – Mineral Resources Management* 25, pp. 189–201.

Kondoro, J.W.A. and Kiwanga, C.A. 1997. Moessbauer study of natural pyrrhotites. *Applied Radiation and Isotopes* 48, pp. 555–563.

Kontny et al. 2000 – Kontny, A., de Wall, H., Sharp, T.G. and Posfai, M. 2000. Mineralogy and magnetic behavior of pyrrhotite from a 260 degrees C section at the KTB drilling site, Germany. *American Mineralogist* 85(10), pp. 1416–1427.

Lambert et al. 1998 – Lambert, J.M., Simkovich, G. and Walker, P.L. 1998. The kinetics and mechanism of the pyrite-to-pyrrhotite transformation. *Metallurgical and Materials Transactions B* 29, pp. 385–396, DOI: 10.1007/s11663-998-0115-x.

Li, H.Y. and Zhang, S.H. 2013. Detection of mineralogical changes in pyrite using measurements of temperature dependence susceptibilities. *Chinese Journal of Geophysics* 48(6), pp. 1384–1391, DOI: 10.1002/cjg2.794.

Mansur et al. 2021 – Mansur, E.T., Barnes, S.J. and Duran, C.J. 2021. An overview of chalcophile element contents of pyrrhotite, pentlandite, chalcopyrite, and pyrite from magmatic Ni-Cu-PGE sulfide deposits. *Mineralium Deposita* 56(1), pp. 179–204, DOI: 10.1007/s00126-020-01014-3.

Matsumoto, K. and Nakamura, M. 2012. Syn-eruptive desulfidation of pyrrhotite in the pumice of the Sakurajima 1914-15 eruption: Implication for potential magma ascent rate meter. *Journal of Mineralogical and Petrological Sciences* 107, pp. 206–211, DOI: 10.2465/jmps.120621b.

Morimoto et al. 1975 – Morimoto, N., Gyobu, A., Tsukuma, K. and Koto, K. 1975. Superstructure and nonstoichiometry of intermediate pyrrhotite. *American Mineralogist* 60, pp. 240–248.

Oliveira et al. 2016 – Oliveira, C.M., Machado, C.M., Duarte, G.W. and Peterson, M. 2016. Beneficiation of pyrite from coal mining. *Journal of Cleaner Production* 139, pp. 821–827, DOI: 10.1016/j.jclepro.2016.08.124.

Palyanova et al. 2019 – Palyanova, G.A., Sazonov, A.M., Zhuravkova, T.V. and Silyanov, S.A. 2019. Composition of pyrrhotite as an indicator of gold ore formation conditions at the sovetskoe deposit (Yenisei Ridge, Russia). *Russian Geology and Geophysics* 60(7), pp. 735–751, DOI: 10.15372/RGG2019049.

Priestley, T. and Paul, B.B. 1964. A thermodynamic study of pyrite and pyrrhotite. *Geochimica et Cosmochimica Acta* 28, pp. 641−671, DOI: 10.1016/0016-7037(64)90083-3.

Selivanov et al. 2011 – Selivanov, E.N., Gulyaeva, R.I. and Vershinin, A.D. 2011. Thermal expansion and phase transformations of natural pyrrhotite. *Inorganic Materials* 44, 438–442, DOI: 10.1134/S0020168508040201.

Shi et al. 2015 – Shi, Y.D., Chen, T.H., Li, P., Zhu, X. and Yang, Y. 2015. The phase transition of pyrite thermal decomposition in nitrogen gas. *Geological Journal of China Universities* 21, pp. 577−583 (*in Chinese*).

Stepanov et al. 2021 – Stepanov, A.S., Large, R.R., Kiseeva, E.S., Danyushevsky, L.V., Goemann, K., Meffre, S., Zhukova, I. and Belousov, I.A. 2021. Phase relations of arsenian pyrite and arsenopyrite. *Ore Geology Reviews* 136, DOI: 10.1016/j.oregeorev.2021.104285.

Tokonami et al. 1972 – Tokonami, M., Nishiguchi, K. and Morimoto, N. 1972. Crystal structure of a monoclinic pyrrhotite (Fe_7S_8). *American Mineralogist* 57(7–8), pp. 1066–1080.

Wang, H.P. and Salveson, I. 2005. A review on the mineral chemistry of the non-stoichiometric iron sulphide, $Fe_{1-x}S$ ($0 \leq x \leq 0.125$): polymorphs, phase relations and transitions, electronic and magnetic structures. *Phase Transitions* 78, pp. 547–567, DOI: 10.1080/01411590500185542.

Wang et al. 2013 – Wang, L., Fan, B.W., He, Y.T., Li, P., Yin, D.Q. and Hu, Y.H. 2013. Characteristics of minerals and their associations of transformation processes in pyrite at elevated temperatures: an X-ray diffraction study. *Ironmaking and Steelmaking* 41(2), pp. 147–152, DOI: 10.1179/1743281213Y.0000000113.

Wang et al. 2008 – Wang, L., Pan, Y.X., Li, J.H. and Qin, H. 2008. Magnetic properties related to thermal treatment of pyrite. *Science in China Series D: Earth Sciences* 51, pp. 1144–1153, DOI: 10.1007/S11430-008-0083-7.

Zhang et al. 2019 – Zhang, Y., Li, Q., Liu, X., Xu, B., Yang, Y. and Jiang, T. 2019. A thermodynamic analysis on the roasting of pyrite. *Minerals* 9(4), DOI: 10.3390/min9040220.

MINERALOGY CHARACTERISTICS, STABILITY CONDITIONS, AND FORMATION PATHWAYS OF SYNTHETIC PYRRHOTITE FORMED BY HEATING PYRITE AT 700°C

Keywords

synthetic pyrrhotite, pyrrhotite, pyrite, hematite

Abstract

Pyrite is a sulfide mineral and is widely distributed in nature. Pyrite may transform into pyrrhotite when heated at high temperatures. In order to support processing engineering techniques and industrial applications of pyrite and pyrrhotite, it is necessary to investigate synthetic pyrrhotite, which is formed by heating pyrite in air, based on existing research. In this work, the mineralogical characteristics and stability conditions of synthetic pyrrhotite formed by heating pyrite at elevated temperatures were studied. The possible formation pathway was verified using a solid-phase reaction. X-ray-diffraction results revealed that synthetic pyrrhotite differs from natural pyrrhotite in the paragenetic association of minerals. Natural pyrrhotite and magnetite coexist in the natural pyrrhotite sample. Synthetic pyrrhotite formed by heating pyrite at 700°C for 1 h has the paragenetic association with hematite and a small amount of pyrite and magnetite. All pyrrhotite samples were monoclinic pyrrhotite-4C (Fe_7S_8) and exhibit minimal differences in terms of lattice parameters. Synthetic pyrrhotite-4C was stable under 0.5–2 h of heating at 700°C in air. It had the highest relative content by heating for 1 h. It was eventually transformed into hematite with heating periods exceeding 3 h, as was the case for pyrite and magnetite. In air, synthetic pyrrhotite-4C is mainly formed via two pathways: (1) pyrite → pyrrhotite-4C and (2) pyrite → magnetite → pyrrhotite-4C. Pathway (1) is more favorable than pathway (2). This transformation cannot be achieved by the reaction between hematite and sulfur.

CHARAKTERYSTYKA MINERALOGICZNA, WARUNKI STABILNOŚCI I ŚCIEŻKI POWSTAWANIA SYNTETYCZNEGO PIROTYNU UTWORZONEGO PRZEZ OGRZEWANIE PIRYTU W TEMPERATURZE 700°C

Słowa kluczowe

pirotyn syntetyczny, pirotyn, piryt, hematyt

Streszczenie

Piryt jest minerałem siarczkowym szeroko rozpowszechnionym w przyrodzie. Piryt może przekształcić się w pirotyn podczas ogrzewania w wysokich temperaturach. W celu wsparcia technik inżynierii mineralnej i przemysłowego zastosowania pirytu i pirotynu, konieczne jest zbadanie syntetycznego pirotynu w oparciu o istniejące badania, który powstaje w wyniku ogrzewania pirytu w powietrzu. W pracy zbadano właściwości mineralogiczne i warunki trwałości syntetycznego pirotynu powstałego w wyniku ogrzewania pirytu w podwyższonej temperaturze. Możliwą ścieżkę powstawania zweryfikowano za pomocą reakcji w fazie stałej. Wyniki dyfrakcji rentgenowskiej ujawniły,

że syntetyczny pirotyn różni się od naturalnego pirotynu w paragenetycznych asocjacjach minerałów. Naturalny pirotyn i magnetyt współistnieją w próbce naturalnego pirotynu. Syntetyczny pirotyn powstały w wyniku ogrzewania pirytu w temperaturze 700°C przez 1 godz. wykazuje asocjację paragenetyczną z hematytem oraz niewielką ilością pirytu i magnetytu. Wszystkie próbki pirotynu były jednoskośnym pirotynem-4C (Fe_7S_8) i wykazują minimalne różnice pod względem parametrów sieci. Syntetyczny pirotyn-4C był stabilny w czasie 0,5–2 godzin ogrzewania w powietrzu w temperaturze 700°C. Najwyższą względną zawartość miał po ogrzewaniu przez 1 godzinę. Ostatecznie został przekształcony w hematyt z okresami ogrzewania przekraczającymi 3 godziny, podobnie jak w przypadku pirytu i magnetytu. W powietrzu syntetyczny pirotyn-4C powstaje głównie dwoma metodami: (1) piryt → pirotyn-4C i (2) piryt → magnetyt → pirotyn-4C. Ścieżka (1) jest korzystniejsza niż ścieżka (2). Tej przemiany nie można osiągnąć w reakcji hematytu z siarką.